

# Fusion studies at around the barrier energies: A case $^{10}\text{B} + ^{27}\text{Al}$ system

Vijay R. Sharma<sup>1,\*</sup>, E. F. Aguilera<sup>1,\*</sup>, P. Amador-Valenzuela<sup>1</sup>, J. C. Morales-Rivera<sup>1</sup>, E. Martinez Quiroz<sup>1</sup> and D. Lizcano

<sup>1</sup>Departamento de Aceleradores, Instituto Nacional de Investigaciones Nucleares, Apartado Postal 18-1027, C.P. 11801, México

E-mail: \*phy.vijayraj@gmail.com, \*eli.aguilera@inin.gob.mx

**Abstract.** Nuclear Reactions around the Coulomb barrier are complex in nature due to the existence of non-fusion channels at these energies, and offers excellent opportunities to explore several dynamical effects as well as the sub-lime effects of nuclear structure. Some of the outstanding issues related to nuclear reactions at these energies are: the role of nucleon transfer events in the manipulation of fusion cross-section, and pairing correlations. As such, an experiment was performed to carry out some conclusive measurements for the  $^{10}\text{B} + ^{27}\text{Al}$  system at energies  $\approx 1.3 - 1.7$  MeV/A. The experiment based on  $\gamma$ -ray spectroscopy has been performed at the Tandem Laboratory, National Institute of Nuclear Investigation, Mexico, to obtain the fusion cross-sections at several beam energies. In the present paper, some experimental details, analysis and preliminary results are presented.

## 1. Introduction

The effect of the break-up mechanism with weakly bound and more recently with radioactive nuclei on the fusion cross-section has become a field of interest for many experimental physicists [1, 2, 3, 4, 5, 6, 7]. Concerning the role of breakup processes in radioactive ion beam (RIB) induced fusion reactions, still it is strenuous to conclude on the associated fusion processes in RIBs without absolute understanding of fusion mechanism in stable nuclei. To have a clear picture on breakup mechanism and the physics of nuclei fragmentation, many physicists paid attention towards fusion studies at energies near the Coulomb barrier with weakly bound stable projectiles, in particular,  $^9\text{Be}$ ,  $^7\text{Li}$  and  $^6\text{Li}$ .

Authors in references [8, 9, 10, 11] reported substantial suppression of complete fusion cross-section for  $^9\text{Be}$ ,  $^7\text{Li}$  and  $^6\text{Li}$  projectiles with  $^{208}\text{Pb}$  and  $^{209}\text{Bi}$  targets at energies above the Coulomb barrier. For the targets ( $^{64}\text{Zn}$  and  $^{59}\text{Co}$ ) in combination with  $^9\text{Be}$ ,  $^7\text{Li}$  and  $^6\text{Li}$  projectiles, fusion cross-sections at energies above barrier were measured and no suppression of total fusion cross-sections were reported by authors [12, 13]. The choice of opting  $^9\text{Be}$ ,  $^7\text{Li}$  and  $^6\text{Li}$  projectiles to investigate the effect of breakup on fusion is because of the low breakup thresholds, ranging from the 1.45 MeV to 2.45 MeV. In the table of nuclides, the nucleus  $^{10}\text{B}$  also has fairly low  $\alpha$ -separation energy ( $S_\alpha$ ) of 4.46 MeV, thereby affecting the fusion mechanism at low bombarding energies. A systematic fusion excitation function measurement carried by Mukherjee et al. [14] for  $^{10}\text{B}$  nuclei with  $^{159}\text{Tb}$  target explains fusion suppression at above barrier energies by  $\sim 14\%$  in frame of coupled channel calculations. As a remark, the onset of the fusion suppression was found to depend on  $\alpha$  breakup threshold of projectiles, i.e., the higher

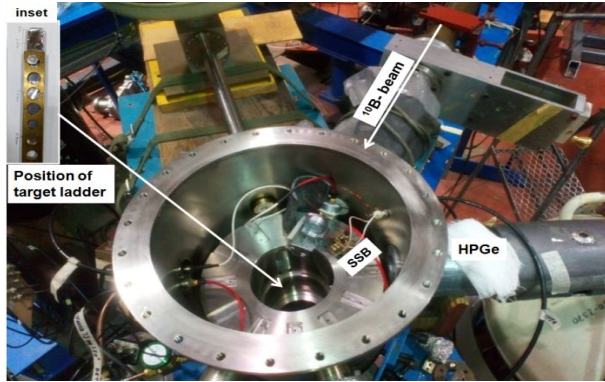


**Figure 1.** (Color Online) A typical snapshot of the experimental setup, in the inset target ladder is shown. For details see text.

the breakup threshold, the higher is the energy where the suppression starts. However, the fusion data for the lighter system  $^7\text{Li}+^{27}\text{Al}$  follow quite well the respective CCDEF predictions [15], which should give realistic model results above the barrier. At most, the higher energy point measured in Ref. [15] shows a very small fusion suppression. Since  $^7\text{Li}$  has a lower separation energy than  $^{10}\text{B}$ , and the energies measured in the present work are smaller than those of Ref. [15], no fusion suppression is expected in the present data. It should be interesting, though, to compare possible below barrier enhancements for these two projectiles.

In the context of above discussed results, it is worth to measure the fusion cross-section for the system with  $^{10}\text{B}$  projectile on low mass targets, in view of the fact that the Coulomb effect ( $Z_P Z_T$ ) can be an important parameterization for understanding the dependency of  $\alpha$  breakup threshold. The present work deals with the measurements of excitation functions (EFs) for  $^{10}\text{B}+^{27}\text{Al}$  system at near and sub barrier energies. Some preliminary results of the measurements are presented herewith.

## 2. Experimental Details

The experiment has been performed using  $^{10}\text{B}^{4+,5+}$  beams from the 6 MV EN Tandem accelerator located in the State of Mexico at National Institute of Nuclear Investigation, Mexico. The target foil of isotopically pure (99.9%) Aluminum was used and the thickness was measured by  $\alpha$ -transmission method and was found to be  $\approx 1.71 \text{ mg/cm}^2$ . This technique is based on the measurement of the energy loss per unit path length by 5.487 MeV  $\alpha$ -particles obtained from a standard  $^{241}\text{Am}$ -source while passing through the target material. Further, the  $^{27}\text{Al}$  foil samples were cut into  $1.2 \times 1.2 \text{ cm}^2$  size and pasted on Stainless Steel holder having concentric hole of 1.0 cm diameter. The irradiation was performed in a scattering chamber of 25 cm diameter at 1.3 - 1.7 MeV/A in steps of 0.5 MeV beam energies at a constant beam current  $\approx 4\text{-}5 \text{ pnA}$ . Typical photograph of the scattering chamber explaining experimental setup consisted of target position, High purity Germanium (HPGe) and a Surface Silicon Barrier (SSB) detectors is shown in figure 1. The purpose to place SSB is to collect information on the back-scattered beam particles, however, HPGe was used to collect the  $\gamma$ -rays emitted by any residual nuclei formed during the reaction. The detector SSB and HPGe were placed at  $150^\circ$  and  $125^\circ$  degrees, respectively, with respect to beam-axis. The activities produced in the sample were recorded online by HPGe and SSB detectors coupled to fast electronic MCA based software Gamma. The detectors used in this experiment were pre-calibrated for energy and efficiency using various standard  $\gamma$ -sources. A typical photo peak efficiency of HPGe detector as a function of  $\gamma$ -ray energies is shown in figure 2(a). On the other hand, the triple alpha source ( $^{239}\text{Pu}/^{241}\text{Am}/^{244}\text{Cm}$ ) spectrum recorded

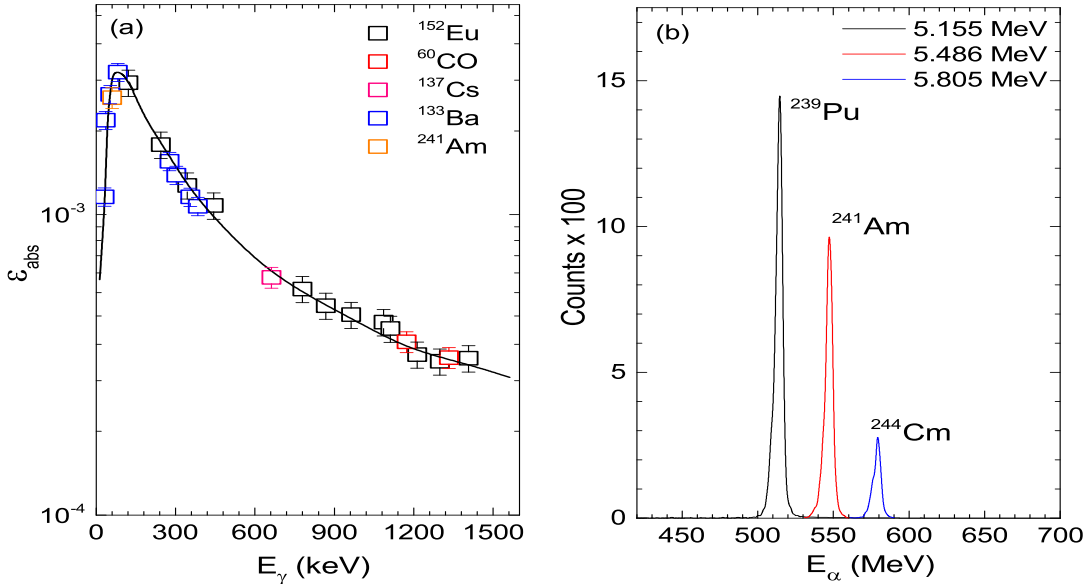


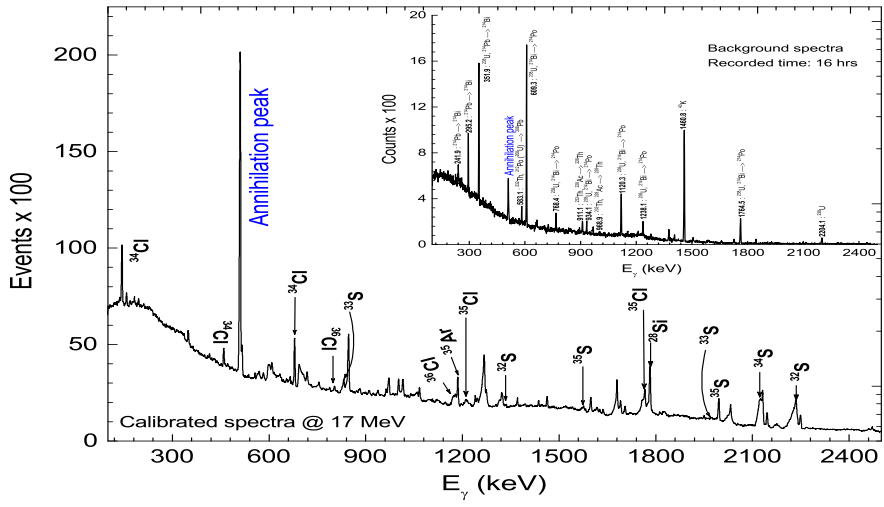
**Figure 2.** (Color Online) (a) A photo peak efficiency curve of HPGe detector as a function of  $\gamma$ -ray energy. The solid line is drawn to guide the eyes. (b) Triple alpha source spectra recorded using SSB detector for calibration purposes.

via SSB detector for calibration purposes is presented in figure 2(b). The reaction residues have been identified by their characteristic  $\gamma$  lines. A typical  $\gamma$ -ray spectrum recorded at projectile energy  $\approx 17$  MeV is shown in figure 3. In this figure, the  $\gamma$  peaks corresponding to different reaction residues are labeled. Off-line data analysis has been performed with the help of data analysis software ROOT [16] developed by CERN.

### 3. Data reduction, Preliminary Results and their interpretations

The measurement and analysis of excitation functions (EFs) can be used to study the reaction mechanism involved in the production of reaction residues. The EFs for  $^{35}\text{Ar}$  (2n),  $^{36}\text{Cl}$  (p),  $^{35}\text{Cl}$  (pn),  $^{35}\text{S}$  (2p),  $^{34}\text{S}$  (2pn),  $^{34}\text{Cl}$  (p2n),  $^{34}\text{Cl}^m$  (p2n),  $^{33}\text{S}$  ( $\alpha$ ),  $^{32}\text{S}$  ( $\alpha$ n),  $^{32}\text{P}$  ( $\alpha$ p),  $^{31}\text{P}$  ( $\alpha$ pn),  $^{29}\text{Si}$  (2 $\alpha$ ),  $^{28}\text{Si}$  (2 $\alpha$ n), and  $^{28}\text{Al}$  (2 $\alpha$ p) radio-nuclides produced in the interaction of  $^{10}\text{B}+^{27}\text{Al}$  system have been measured. It may be mentioned that the prompt  $\gamma$ -rays and delayed  $\gamma$ -rays (via activation technique) emitted by the reaction residues were considered to determine the absolute fusion cross-section which were measured using standard equation as discussed in reference [17, 18]. The energy loss in the target is accounted as described in Ref. [19]. Further, a constant normalization in the absolute cross-section has been done for all the observed reaction residues and at all studied energies using Sao Paulo Potential [20]. The fact that the measured absolute cross-sections were considerably underpredicted when compared with the Sao Paulo Potential calculations and might be due to some constant normalization factor related to either beam integration or absolute efficiency calibration. It is important to note that additional measurements will be performed to establish the correct normalization factor.

In the present work, the experimental EFs have been analysed in the framework of equilibrated compound nucleus ( $^{37}\text{Ar}$ ) decay using statistical model code PACE2 [21]. The code PACE2 is based on the Hauser-Feshbach approach of compound nucleus (CN) de-excitation.



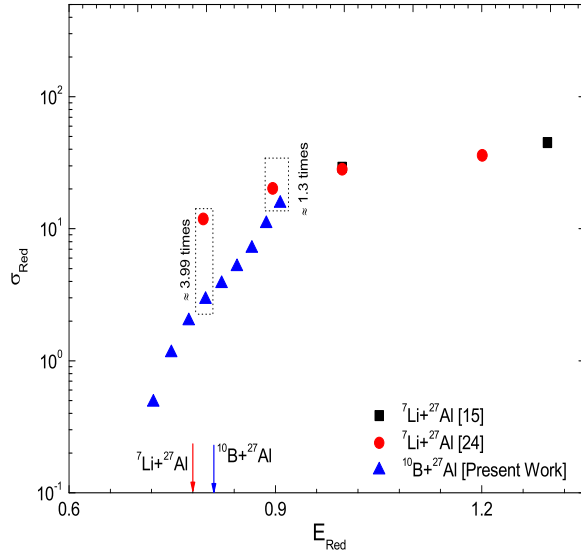


**Figure 5.** (Color Online) Fusion excitation function plotted by using normalization procedure. For details see text.

The production cross-sections of evaporation residues are calculated using the Bass formula, and the de-excitation of CN is followed by a Monte Carlo procedure. As explained in Ref. [22], we have updated our PACE2 version to use the AME12 mass table [23]. For an instance, the measured EFs for the 2n, pn, p2n,  $\alpha$ ,  $\alpha$ pn and 2 $\alpha$ n channels alongwith the predictions of PACE2 using physically reasonable parameters are shown in figure 4 (a and b). As can be seen in the figure 4(a), the experimentally measured cross-sections for  $^{35}\text{Cl}$  populated via pn channel is found to be reproduced by statistical model prediction at above barrier energies ( $E_{Lab} > V_B \approx 14.01$  MeV), which indicates its production through complete fusion mode only, on the other hand, at barrier and below barrier energies the experimental cross-section is over predicted by the PACE2 code indicating a possible involvement of another dominating mechanism. In case of  $^{35}\text{Ar}$  and  $^{34}\text{Cl}$  populated via 2n and p2n channels respectively, the experimental cross-section is over predicted (for 2n channel) and under-predicted (for p2n channel) by statistical model indicating mechanism like pre-equilibrium process or the coupling to some direct channel process trying to interplay at the studied energy range. Some high energy  $\gamma$ -lines falling in the low efficiency region of the detector might be missing in the data, but further investigation is needed to elucidate this point. Similar observations can be noticed in figure 4 (b) for  $^{28}\text{Si}$  populated via 2 $\alpha$ n and for  $^{33}\text{S}$  populated via  $\alpha$ , the experimental cross-section is over predicted by the statistical calculations, therefore we suppose that there might be an interplay of other possible nuclear mechanism like transfer (i.e. formation of  $^{28}\text{Si}$  residue via reactions (i)  $^{10}\text{B} + ^{27}\text{Al} \rightarrow ^{28}\text{Si} + 2\alpha$ n, or (ii)  $^{10}\text{B} + ^{9}\text{Be} + ^{27}\text{Al} \rightarrow ^{28}\text{Si} + ^{9}\text{Be}$ ), or incomplete fusion (i.e. formation of  $^{33}\text{S}$  via reaction  $^{10}\text{B} + ^{6}\text{Li} + \alpha + ^{27}\text{Al} \rightarrow ^{33}\text{S} + \alpha$ ). Since, the code PACE2 only considers the CF mechanism, it is important to extend statistical calculations using CCFULL, CRC and DWBA (FRESCO) methods.

In order to compare the behavior of measured reaction cross-section with the available data for  $^{7}\text{Li} + ^{27}\text{Al}$  system [24, 15], a reduced fusion cross-section ( $\sigma_{Red} = (\sigma_R / (A_P^{1/3} + A_T^{1/3}))^2$ ) and

reduced projectile energy ( $E_{Red} = E_{CM} \cdot (A_P^{1/3} + A_T^{1/3}) / (Z_P \cdot Z_T)$ ) in center of mass frame technique is used [25] and is presented in figure 5. As can be seen in the figure, that the reduced reaction cross section for the projectile  $^7\text{Li}$  is  $\approx 1.3$  times higher at  $E_{Red} \approx 0.89$  and increases to  $\approx 3.99$  times at  $E_{Red} \approx 0.79$ ; this result is compatible with the concept that the smaller the threshold break-up energy, the larger the reaction cross section, but one must have in mind that the present results are still preliminary. A final conclusion will be drawn after the complete analysis of the present work is performed.

#### 4. Summary and Conclusions

An experiment to measure the fusion cross-sections for  $^{10}\text{B} + ^{27}\text{Al}$  system at energies below and above the barrier was performed. Within a frame of PACE2 predictions, the experimental measured cross-sections were compared for the observed reaction channels populated via  $\text{xn}$ ,  $\text{pxn}$ ,  $\alpha$  and  $2\alpha$  evaporation channels. In case of  $^{28}\text{Si}$  and  $^{33}\text{S}$ , the observed enhancement of cross-sections over the predictions of statistical model calculations obtained using the code PACE2 may be attributed to the transfer or complete fusion of the projectile. It is important to perform the corresponding calculations to confirm these points.

#### 5. Acknowledgments

The author VRS and EFA thank CONACYT for providing financial support under Project No. CB-01-254619.

#### References

- [1] N. Takigawa et al., Phys. Rev. C 47 (1993) R2470.
- [2] C. H. Dasso, A. Vitturi, Phys. Rev. C 50 (1994) R12; C.H. Dasso, A. Vitturi, Nucl. Phys. A 597 (1996) 473.
- [3] M. Hussein et al., Phys. Rev. C 48 (1992) 377; M. Hussein et al., Phys. Rev. Lett. 72 (1994) 2693; M. Hussein et al., Nucl. Phys. A 588 (1995) 85c.
- [4] J. Takahashi et al., Phys. Rev. Lett. 78 (1997) 30.
- [5] K. J. Cook, E. C. Simpson et al. Phys. Rev. Lett. 122 (2019) 102501.
- [6] E. F. Aguilera et al., Phys. Rev. C 93 (2016) 034613
- [7] F. D. Becchetti, J. J. Kolata and TwinSol Collaboration, Nuclear Instruments and Methods in Phys. R Section B, Volume 376, 397-401 (2016).
- [8] M. Dasgupta, et al., Phys. Rev. Lett. 82 (1999) 1395.
- [9] C. Signorini, et al., Eur. Phys. J. A 5 (1999) 7.
- [10] M. Dasgupta, et al., Phys. Rev. C 66 (2002) 041602(R).
- [11] M. Dasgupta, et al., Phys. Rev. C 70 (2004) 024606, and references therein.
- [12] S. B. Moraes, et al., Phys. Rev. C 61 (2000) 064608.
- [13] C. Beck, et al., Phys. Rev. C 67 (2003) 054602.
- [14] A. Mukherjee et al., Physics Letters B 636 (2006) 9195.
- [15] K. Kalita et al, Phys. Rev. C 73, (2006) 024609.
- [16] I. Antcheva, M.Ballintijn, B.Bellenot, M.Biskup, R.Brun et al., Computer Physics Communications; Anniversary Issue, Volume 180, Issue 12, 2499-2512 (2009).
- [17] E. F. Aguilera, Ph.D. Thesis, Department of Physics, University of Notre Dame, 1985.
- [18] V. R. Sharma et al., Phys. Rev. C 89 (2014) 024608.
- [19] E. F. Aguilera et al., Phys. Rev. C 41 (1990) 910-919.
- [20] L. C. Chamon, Nuclear Physics A, Vol. 787, Issues 14, Pages 198-205, (2007).
- [21] A. Gavron Phys. Rev. C 21, (1980) 230.
- [22] E. F. Aguilera et al., Phys. Rev. C 93, (2016) 034613.
- [23] M. Wang et al., Chinese Phys. C 36, (2012) 1603.
- [24] D. Patel et al., Pramana, Vol. xx, No. x, (2013) 1-16.
- [25] P. R. S. Gomes et al., Physical Rev. C 71,(2005) 017601.